Entanglement trapping in a nonstationary structured reservoir

C. Lazarou,[1] K. Luoma,[2] S. Maniscalco,[2,3] J. Piilo,[2] and B. M. Garraway[4]

[1]*Department of Physics and Astronomy, University College London, Gower Street, London WC1E-6BT, United Kingdom*

[2]*Turku Centre for Quantum Physics, Department of Physics and Astronomy, University of Turku, FI-20014 Turun yliopisto, Finland*

[3]*SUPA, Department of Physics, Heriot-Watt University, Edinburgh, EH14 4AS, United Kingdom*

[4]*Department of Physics and Astronomy, University of Sussex, Falmer, Brighton, BN1 9QH United Kingdom*

(Received 22 May 2012; published 27 July 2012)

We study a single two-level atom interacting with a reservoir of modes defined by a reservoir structure function with a frequency gap. Using the pseudomodes technique, we derive the main features of a trapping state formed in the weak coupling regime. Utilizing different entanglement measures we show that strong correlations and entanglement between the atom and the modes are in existence when this state is formed. Furthermore, an unexpected feature for the reservoir is revealed. In the long time limit and for weak coupling the reservoir spectrum is not constant in time.

DOI: 10.1103/PhysRevA.86.012331 PACS number(s): 03.67.Mn, 03.65.Yz, 03.67.Bg

I. INTRODUCTION

In recent years, entanglement and quantum correlations have attracted the attention of many physicists working in the area of quantum mechanics [1,2]. This is due to the ongoing research in the area of quantum information [3] and also because of the advances made in different experimental disciplines, such as in ion traps [4] and Bose-Einstein condensation [5,6]. Developments in the field of cavity QED, where experiments in the strong coupling regime are carried out [7,8], provide plenty of motivation for studying quantum information and entanglement. Theoretical studies are also important in the context of atom-light interactions inside structured reservoirs [9], such as resonant cavities or photonic band gap materials. The theoretically predicted atom-photon bound state could also lead to entanglement and this can also be linked to another problem: that of atom-laser out-coupling from Bose-Einstein condensates [10–12], where analogous effects were predicted in the past.

When quantifying entanglement between an atom and a reservoir of modes, the modes can be treated collectively [13]. The system is described in terms of two subsystems and one can use existing bipartite entanglement measures. This, of course, does not permit the study of entanglement between individual reservoir modes. It is also possible to partition the reservoir and then quantify entanglement between different parts of the reservoir [14]. A different approach is that offered by a recently proposed measure, the density of entanglement [15]. This measure quantifies entanglement between the atom and different modes in terms of time-dependent distributions.

The problem of entanglement between an atom and a bath of modes is becoming more interesting when considering reservoirs with a spectral gap in their densities of states. For such systems, it is well known that an atom-photon bound state can be formed [9,16–22]. In view of this result, it is reasonable to expect strong quantum correlations and entanglement between the atom and the reservoir.

Motivated by this we consider here a two-level atom coupled to a model reservoir with a single frequency gap in its density of modes. Exploring the dynamics at different coupling regimes, we are able to show that when a trapping state is formed, permanent correlations are observed. Using the pseudomodes technique [23,24], and a tripartite entanglement measure, the tangle [25], we quantify and study the properties of entanglement. Furthermore, a careful analysis reveals that in the long time limit and when a trapping state is formed, the reservoir spectrum is not constant in time. This is due to a continuous coupling between the atom and individual modes, which has zero net energy flow, but induces a permanent effective coupling between the reservoir modes. In terms of the pseudomode description, the population trapping arises because of the dark state between the atom and one of the pseudomodes.

This paper is organized as follows. In Sec. II, we introduce the model and the pseudomodes method. In Sec. III, we discuss the formation of the trapping state and the reservoir dynamics in the long time limit. In Sec. IV, an analysis of entanglement dynamics in terms of the tangle and the density of entanglement is presented. We conclude in Sec. V, and in the Appendix a synopsis of the pseudomodes method is provided.

II. MODEL

The system we consider in this work, consists of a two-level atom coupled to a reservoir of harmonic oscillators with annihilation and creation operators $\hat{a}_\lambda$ and $\hat{a}_\lambda^\dagger$, respectively. Within the rotating wave approximation, the Hamiltonian reads ($\hbar = 1$)

$$H = \sum_\lambda \omega_\lambda \hat{a}_\lambda^\dagger \hat{a}_\lambda + \omega_0 |1_a\rangle\langle 1_a| + \sum_\lambda g_\lambda (\hat{a}_\lambda^\dagger |0_a\rangle\langle 1_a| + \hat{a}_\lambda |1_a\rangle\langle 0_a|), \quad (1)$$

where g_λ is the coupling between the mode λ and the atomic transition $|1_a\rangle \rightarrow |0_a\rangle$. The atomic transition frequency is ω_0, whereas the λ-mode frequency is ω_λ.

For the purposes of the analysis that follows, it is very useful to introduce the reservoir structure function $D(\omega_\lambda)$, which reflects the properties of the density of modes [23]. This is defined through

$$\rho_\lambda (g_\lambda)^2 = \frac{\Omega_0^2}{2\pi} D(\omega_\lambda), \quad (2)$$

and is normalized such that

$$\int_{-\infty}^{\infty} d\omega D(\omega) = 2\pi. \tag{3}$$

With this normalization, a measure of the overall coupling strength is Ω_0, which is given by

$$\Omega_0^2 = \sum_{\lambda} (g_\lambda)^2. \tag{4}$$

In Eq. (2), ρ_λ is the density of modes, i.e., the number of modes with frequencies in the interval ω_λ to $\omega_\lambda + \mathrm{d}\omega_\lambda$.

Previous studies revealed that the formation of an atom-photon bound state is plausible, when an atom is coupled to a reservoir with a gap in its structure function [9,16–22]. It has also been suggested that the formation of such a bound state is an indication of entanglement between the atom and its environment [26,27]. In order to explore entanglement dynamics between an atom and a reservoir with a gap at a given frequency ω_c, we utilize the following structure function for the reservoir:

$$D(\omega) = W_1 \frac{\Gamma_1}{(\omega-\omega_c)^2+(\Gamma_1/2)^2} - W_2 \frac{\Gamma_2}{(\omega-\omega_c)^2+(\Gamma_2/2)^2}. \tag{5}$$

This superposition of Lorentzians with the same center frequency ω_c, widths Γ_j, amplitudes W_j, and opposite signs will result in a gap, i.e., $D(\omega_c) = 0$, if $\Gamma_1 W_2 = \Gamma_2 W_1$. Because of the normalization condition Eq. (3), we also have that $W_1 - W_2 = 1$.

Starting with the atom initially excited and the reservoir in the vacuum state, one has to solve the Schrödinger equation to obtain the system dynamics for $t > 0$. This can be done either with analytical methods, e.g., the Laplace transform [20,22], or numerical integration [9,16,17]. An alternative approach is that offered by the pseudomodes method [23,24].

According to this method, the reservoir modes are replaced by two degenerate pseudomodes [23,24]; see Fig. 1. The two pseudomodes are interacting with each other, while one of them is also coupled to the atom. Finally, the two pseudomodes decay at rates Γ_1' and Γ_2', respectively.

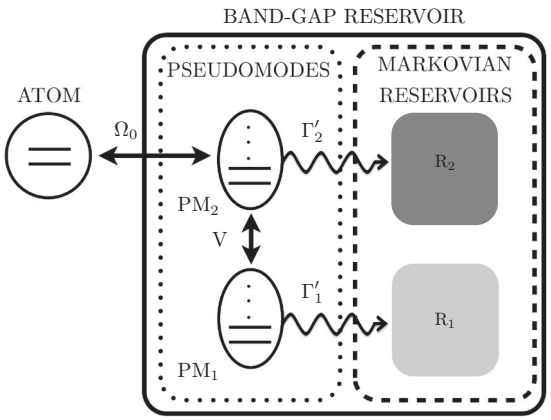

FIG. 1. Diagrammatic representation of the atom-pseudomodes system. The band-gap reservoir is represented by two interacting pseudomodes PM_1 and PM_2. The two pseudomodes are also coupled to two independent Markovian reservoirs that induce the decay of the pseudomodes at rates Γ_1' and Γ_2', respectively. The atom couples only to one of the two pseudomodes. For a perfect gap, i.e., $D(\omega_c) = 0$, the decay rate for the first pseudomode Γ_1' is zero.

The dynamics of the system are described by a Markovian master equation [23,24]

$$\dot{\rho}(t) = -i\,[H_0, \rho(t)] - \sum_{j=1}^{2} \frac{\Gamma_j'}{2} [\hat{a}_j^\dagger \hat{a}_j \rho(t) - 2\hat{a}_j \rho(t) \hat{a}_j^\dagger + \rho(t) \hat{a}_j^\dagger \hat{a}_j], \tag{6}$$

with the Hamiltonian

$$\begin{aligned} H_0 = {} & \omega_0 |1_a\rangle\langle 1_a| + \omega_c (\hat{a}_1^\dagger \hat{a}_1 + \hat{a}_2^\dagger \hat{a}_2) \\ & + \Omega_0 (\hat{a}_2^\dagger |0_a\rangle\langle 1_a| + \hat{a}_2 |1_a\rangle\langle 0_1|) \\ & + V (\hat{a}_1^\dagger \hat{a}_2 + \hat{a}_1 \hat{a}_2^\dagger), \end{aligned} \tag{7}$$

where $\hat{a}_1$ ($\hat{a}_1^\dagger$) and $\hat{a}_2$ ($\hat{a}_2^\dagger$) are the annihilation (creation) operators for the two pseudomodes, respectively. The vacuum and excited states for the atom are $|0_a\rangle$ and $|1_a\rangle$. The coupling Ω_0 is given by Eq. (4), and $V = \sqrt{W_1 W_2}(\Gamma_1 - \Gamma_2)/2$. The two decay rates are $\Gamma_1' = W_1\Gamma_2 - W_2\Gamma_1$ and $\Gamma_2' = W_1\Gamma_1 - W_2\Gamma_2$. For a perfect gap $D(\omega_c) = 0$, the decay rate for the first pseudomode is $\Gamma_1' = 0$, $\Gamma_2' = (\Gamma_1 + \Gamma_2)$, and $V = \sqrt{\Gamma_1\Gamma_2}/2$.

The solution for the master equation (6) reads

$$\rho(t) = \Pi_j(t) |0_a 0_1 0_2\rangle\langle 0_a 0_1 0_2| + |\tilde{\psi}(t)\rangle\langle\tilde{\psi}(t)|, \tag{8}$$

where

$$|\tilde{\psi}(t)\rangle = c_a(t)|1_a 0_1 0_2\rangle + a_1(t)|0_a 1_1 0_2\rangle + a_2(t)|0_a 0_1 1_2\rangle. \tag{9}$$

The vacuum state $|0_a 0_1 0_2\rangle$ population is $\Pi_j(t)$, and the probability amplitudes for the atom and the first and second pseudomodes are $c_a(t)$, $a_1(t)$, and $a_2(t)$, respectively. A synopsis of the pseudomode method is provided in the Appendix, along with the expressions for the probability amplitudes $c_a(t)$, $a_1(t)$, and $a_2(t)$ and the population $\Pi_j(t)$.

III. POPULATION TRAPPING AND NONSTATIONARY ENVIRONMENT

For a resonant system $\omega_c = \omega_0$, and when the perfect gap condition $\Gamma_1 W_2 = \Gamma_2 W_1$ is met, we have that $D(\omega_c) = 0$, and in the long time limit a trapping state is formed [24]. Upon solving the equations for $c_a(t)$, $a_1(t)$, and $a_2(t)$ (see Appendix), and taking their limits for $t \to \infty$, we have that

$$c_a(\infty) = (1+\eta^2)^{-1}, \tag{10}$$

and

$$a_1(\infty) = \eta(1+\eta^2)^{-1}, \tag{11}$$

where $\eta = 2\Omega_0/\sqrt{\Gamma_1\Gamma_2}$. The probability amplitude for the second pseudomode is $a_2(\infty) = 0$ and the population of the vacuum state is

$$\Pi_j(\infty) = \eta^2(1+\eta^2)^{-1}. \tag{12}$$

A plot of $|c_a(t)|^2$, $|a_1(t)|^2$, $|a_2(t)|^2$, and $\Pi_j(t)$ for $\Gamma_1 = 10\Omega_0$ and $\Gamma_2 = 0.2\Omega_0$ is shown in Fig. 2(a).

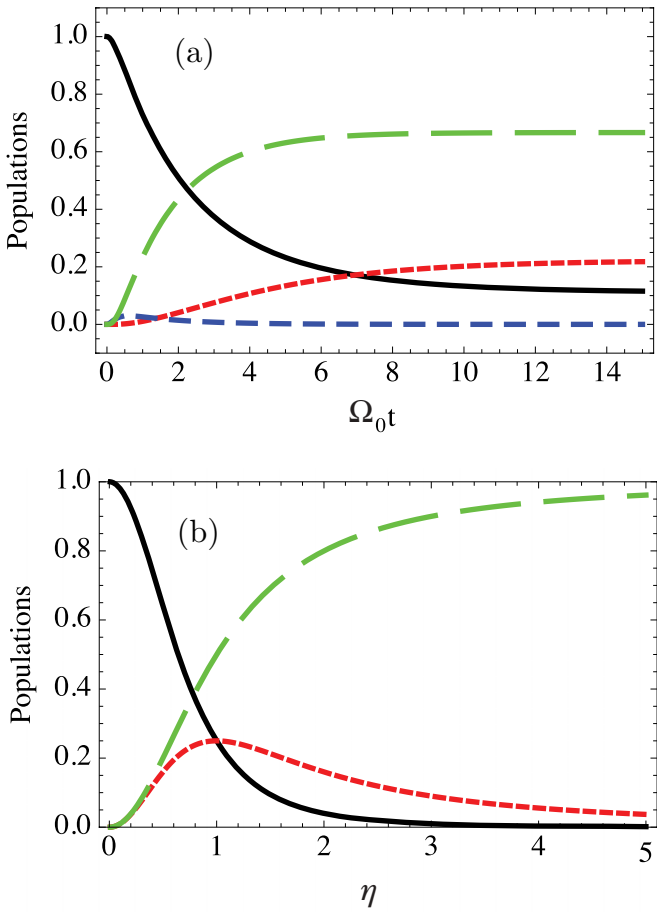

FIG. 2. (Color online) (a) The populations $|c_a(t)|^2$ (black), $|a_1(t)|^2$ (red short-dashed), $|a_2(t)|^2$ (blue dashed), and $\Pi_j(t)$ (green long-dashed), for $\Gamma_1 = 10\Omega_0$, $\Gamma_2 = 0.2\Omega_0$, and $W_1 = 50W_2$. (b) The final populations $|c_a(\infty)|^2$ (black), $|a_1(\infty)|^2$ (red short-dashed), and $\Pi_j(\infty)$ (green-dashed) as functions of the dimensionless parameter $\eta = 2\Omega_0/\sqrt{\Gamma_1\Gamma_2}$.

From the above three equations it is evident that in the long time limit, and in the weak coupling regime $\eta \ll 1$, a fraction of the population will remain trapped in the excited atomic state and the second pseudomode; see Fig. 2(b). The remaining population is irreversibly lost to the reservoir (or more precisely, to the Markovian part of the reservoir [28]). From Fig. 2(b) and Eqs. (10)–(12) we can see that population trapping, i.e., $|c_a(\infty)|^2$, is significant for $\eta \leqslant 1$. The population lost to the reservoir, i.e., the sum of the populations for the pseudomode 1 $|a_1(\infty)|^2$ and the vacuum state $\Pi_j(t)$, remains low for $\eta \ll 1$; see Fig. 2(b). As we move to the strong coupling regime $\eta \geqslant 1$ losses increase, and eventually for $\eta \gg 1$ all the population is transferred to the reservoir.

An interesting feature of the trapping state is that in the long time limit the reservoir modes do not reach a steady state. This can be evidenced in the reservoir spectrum for $t \to \infty$. Using the definition for the reservoir spectrum [29],

$$S(\omega_\lambda,t) = \rho_\lambda |c_\lambda(t)|^2, \tag{13}$$

and Eq. (A17) for $t(\Gamma_1 + \Gamma_2) \gg 1$, we get the following expression for $S(\omega_\lambda,t)$:

$$S(\omega_\lambda,t) = \frac{8\Omega_0^2 D(\omega_\lambda)}{\pi(4\Gamma^2+\Omega^2)^2}\left|\frac{\Gamma_1\Gamma_2}{2\delta_\lambda}e^{i\delta_\lambda t/2}\sin\left(\frac{\delta_\lambda t}{2}\right) + \frac{4\Omega_0^2(2\Gamma - i\delta_\lambda)}{4(\Gamma - i\delta_\lambda)^2+\Omega^2}\right|^2, \tag{14}$$

where the width Γ and the Rabi frequency Ω are given in Eqs. (A14) and (A15), and $\delta_\lambda = \omega_\lambda - \omega_c$.

Thus, in the long time limit, although the total excitation in the reservoir is constant, the modes remain coupled to each other. As a result of this the population distribution between the modes changes; see Fig. 3. The oscillatory exchange of population between the modes is more pronounced in the weak coupling regime $\Omega_0 \ll \sqrt{\Gamma_1\Gamma_2}$ [Fig. 3(a)] and is negligible for the strong coupling regime [Fig. 3(b)]. Snapshots of the reservoir spectrum for times $t(\Gamma_1 + \Gamma_2) \gg 1$ are shown in Figs. 3(c) and 3(d). It is also interesting to note that in the weak coupling regime displaying the population trapping, the frequency gap imposes strong oscillations in the mode populations compared to the single Lorentzian structure function case [15]; see Fig. 3(c). In contrast with strong coupling and no population trapping, there is a strong resemblance in the mode populations between the gap and single Lorentzian cases [Fig. 3(d)].

In order to explore further these features, we plot in Fig. 4(a) the probability current between the atom and the λ mode [30,31],

$$J_{\lambda,a}(t) = 2\mathrm{Im}\{\rho_\lambda g_\lambda \tilde{c}_\lambda^*(t)\tilde{c}_a(t)e^{i\delta_\lambda t}\}, \tag{15}$$

and in Fig. 4(b) the net probability current,

$$Q(t) = \int_{-\infty}^{\infty} d\omega_\lambda J_{\lambda,a}(t). \tag{16}$$

The long time limit, i.e., when $t \to \infty$, is of particular interest. We see that while the net probability current Fig. 4(b) approaches zero, in the long time limit, the individual reservoir frequency components seen in Fig. 4(a) do not decay but continue oscillating. This does not happen in the case of a Lorentzian reservoir coupling and appears to be a feature of population trapping in a photonic band-gap structure. Subsequently, there exists an effective, atom-mediated coupling between the modes even though the atom has reached a steady state.

For reservoirs with a single Lorentzian structure function, the pseudomodes method has provided an intuitive insight into memory effects [28]. When an atom is coupled to such an environment, slowly decaying oscillations between the atom and the reservoir are observed in the strong coupling limit [15,28]. These correlation effects are attributed to a memory part of the reservoir that is represented by a single pseudomode. The rest of the reservoir acts as a Markovian environment that induces a slow exponential decay for the memory part.

In the current system with a frequency gap in the environment, we have two pseudomodes that store information about the state of the atom. The first one, $a_1(t)$, i.e., the one that forms the trapping state with the atom, is responsible for the permanent storage of information. The second one, $a_2(t)$, is

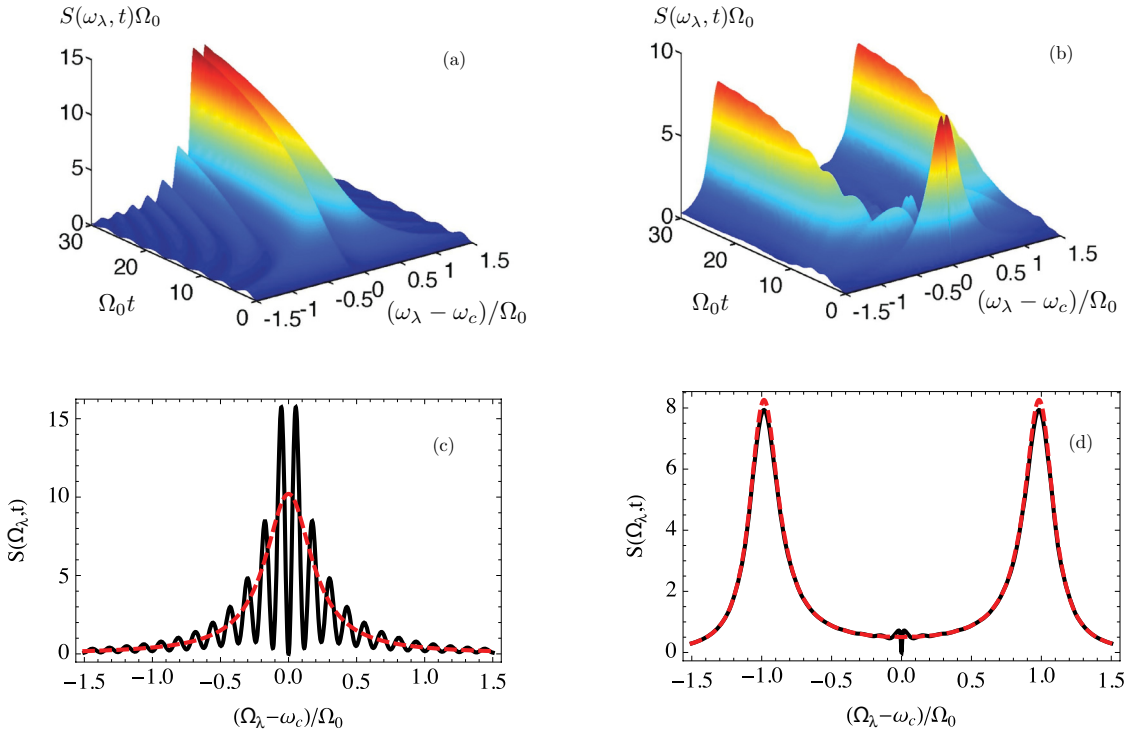

FIG. 3. (Color online) The reservoir spectrum $S(\omega_\lambda,t)$ as a function of time, (a) for $\Gamma_1 = 10\Omega_0$, $\Gamma_2 = 0.2\Omega_0$, and $W_1 = 50W_2$, and (b) for $\Gamma_1 = 0.5\Omega_0$, $\Gamma_2 = 0.01\Omega_0$, and $W_1 = 50W_2$. Panels (c) and (d) are snapshots for the reservoir spectrum for $\Omega_0 t = 50$ and for the parameters of panels (a) and (b), respectively. The red dashed line in panels (c) and (d) is the spectrum for a reservoir with a Lorentzian structure function with $\Gamma_2 = W_2 = 0$, $W_1 = 1$ and $\Gamma_1 = 10\Omega_0$ and $\Gamma_1 = 0.5\Omega_0$, respectively.

responsible for short-term storage but eventually gets depleted due to its coupling to the rest of the reservoir. Though the atom is directly coupled to the second pseudomode only, the interaction between the pseudomodes gives rise to the trapping of population by forming a dark state for the atom-pseudomode one subsystem.

In general, the population trapping signifies the formation of an atom-photon bound state. In view of the strong permanent correlation effects that dictate the formation of such a state, it is reasonable to expect entanglement to be also present. In the following section we use both the pseudomodes method and the recently proposed density of entanglement [15] to explore entanglement between the atom and the reservoir defined by Eq. (5).

IV. ENTANGLEMENT DYNAMICS

Identifying and measuring entanglement in multipartite systems presents various complications. Apart from the case of a two-qubit system, where entanglement can be identified both for a pure and a mixed state [32,33], multiqubit entanglement is an open problem and to date several measures of entanglement have been proposed [1,2,15,25,34–37]. For the analysis that follows, we will be using two different measures [15,25].

The first one, called tangle [25], is a measure of genuine tripartite entanglement between three qubits. This will be used to explore entanglement dynamics in the pseudomodes framework. The second one is the recently proposed density of entanglement [15]. This measure is appropriate for studying entanglement between an atom and the continuum of the reservoir modes. It provides valuable information regarding entanglement distribution between the atom and the modes and between individual modes.

A. Tangle

We start our analysis from Eqs. (8) and (9), i.e., the density matrix for the atom-pseudomodes system. For this mixed state, the two pseudomodes can be collectively described in terms of a single qubit. The two states for this collective qubit are

$$|0_{\rm ps}\rangle = |0_1 0_2\rangle, \tag{17}$$

and

$$|1_{\rm ps}\rangle = \frac{1}{\sqrt{|a_1(t)|^2 + |a_2(t)|^2}} \left[a_1(t)|1_1 0_2\rangle + a_2(t)|0_1 1_2\rangle\right]. \tag{18}$$

Using these expressions, the state $|\tilde{\psi}(t)\rangle$ reads

$$|\tilde{\psi}(t)\rangle = c_a(t)|1_a 0_{\rm ps}\rangle + \sqrt{|a_1(t)|^2 + |a_2(t)|^2}|0_a 1_{\rm ps}\rangle, \tag{19}$$

and the density matrix $\rho(t)$ becomes

$$\rho(t) = \Pi_j(t)|0_a 0_{\rm ps}\rangle\langle 0_a 0_{\rm ps}| + |\tilde{\psi}(t)\rangle\langle\tilde{\psi}(t)|. \tag{20}$$

We should note here, that the states $|0_{\rm ps}\rangle$ and $|1_{\rm ps}\rangle$ are both eigenstates with zero eigenvalues for the reduced density matrix $\rho_{12}(t) = {\rm tr}_a\{\rho\}$ for the two pseudomodes, where the tracing is over the atomic states $|0_a\rangle$ and $|1_a\rangle$.

Entanglement for this "two-qubit" mixed state can be quantified in terms of the concurrence [32,33]. This can be associated with tangle, a measure of tripartite entanglement

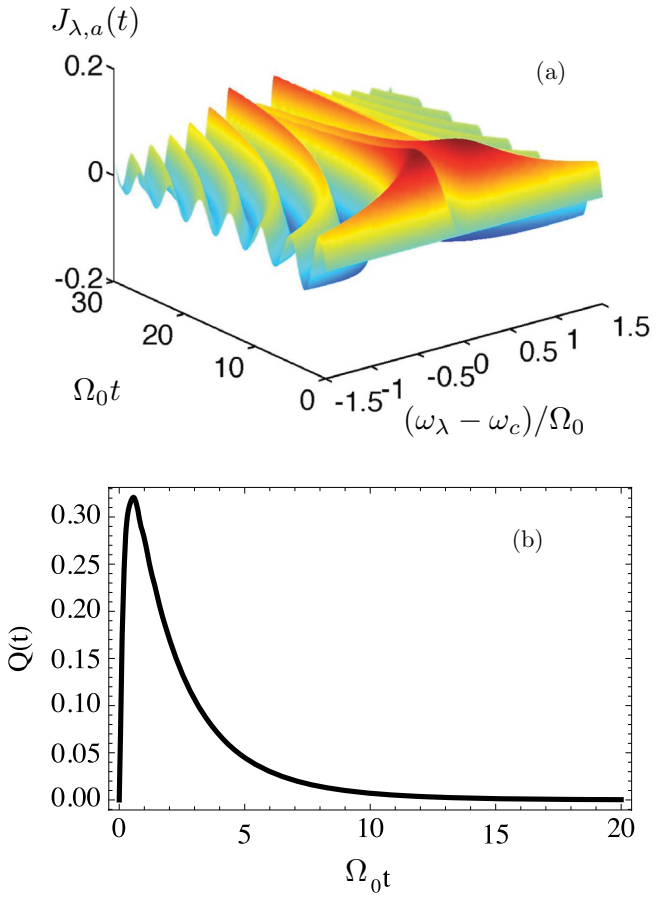

FIG. 4. (Color online) (a) The probability current $J_{\lambda,a}(t)$ [Eq. (14)], for $\Gamma_1 = 10\Omega_0$, $\Gamma_2 = 0.2\Omega_0$, and $W_1 = 50W_2$, and (b) the total probability current $Q(t)$ [Eq. (15)] for the same parameters.

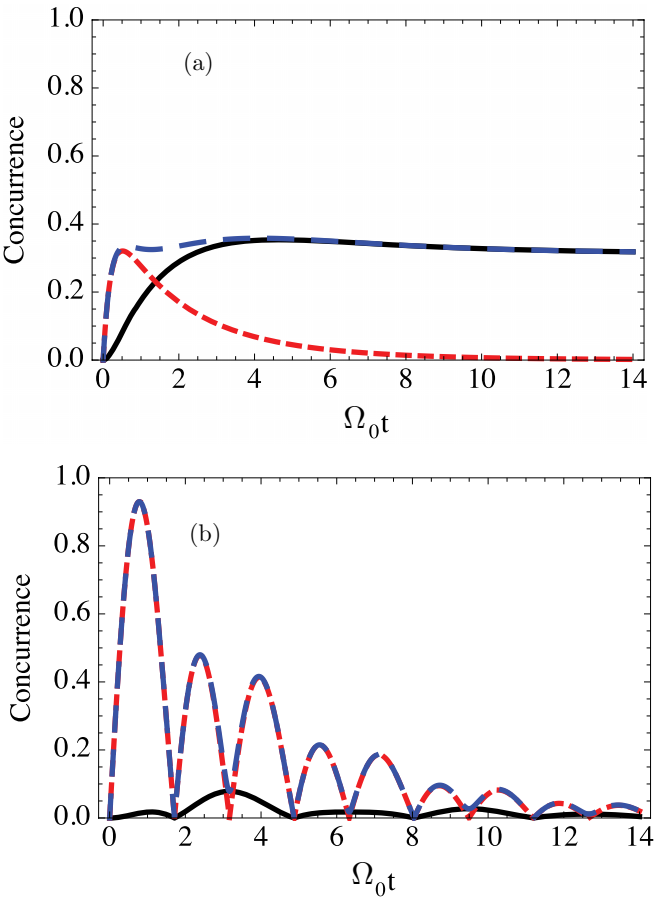

FIG. 5. (Color online) The concurrences $C_{a,1}(t)$ (black solid), $C_{a,2}(t)$ (red short-dashed), and $C_{a,(12)}(t)$ (blue dashed), for (a) $\Gamma_1 = 10\Omega_0$, $\Gamma_2 = 0.2\Omega_0$, and for (b) $\Gamma_1 = 0.5\Omega_0$, $\Gamma_2 = 0.01\Omega_0$. For both panels $W_1 = 50W_2$.

for a system of three qubits A, B, and C [25]. The tangle τ_{ABC} expressed in terms of pairwise concurrences reads

$$\tau_{ABC} = C^2_{A(BC)} - C^2_{AB} - C^2_{AC} \tag{21}$$

where C_{AB} and C_{AC} are the pairwise concurrences for the qubit A with B and C, respectively, whereas $C_{A(BC)}$ is the concurrence for qubit A and a qubit (BC) that collectively describes qubits B and C.

The above equation can also be written as an inequality, i.e.,

$$C^2_{A(BC)} \geqslant C^2_{AB} + C^2_{AC}. \tag{22}$$

The meaning of these two equations is that entanglement between the qubit A and the other two qubits, B and C, is manifested through direct entanglement with each qubit, thus the two concurrences C_{AB} and C_{AC}, and through a three-way (tripartite) entanglement, i.e., τ_{ABC}.

From the three qubit density matrix Eq. (8), we derive the reduced density matrices for the atom with each individual pseudomode, i.e., $\rho_{a,1}$ and $\rho_{a,2}$. Using the concurrence for a two-qubit system [32,33] we obtain the following two expressions for the concurrence for the atom with each pseudomode:

$$C^2_{a,1}(t) = 4|c_a(t)|^2|a_1(t)|^2, \tag{23}$$

and

$$C^2_{a,2}(t) = 4|c_a(t)|^2|a_2(t)|^2. \tag{24}$$

The final step is to calculate the concurrence for the density matrix Eq. (20).

This is the concurrence for the atom and the qubit that collectively describes the two pseudomodes. The calculation is simple and the concurrence $C^2_{a,(12)}(t)$ is

$$C^2_{a,(12)}(t) = C^2_{a,1}(t) + C^2_{a,2}(t), \tag{25}$$

i.e., the tangle for the atom and the two pseudomodes is zero. From the definition of the tangle, Eqs. (21) and (22), and the above result, we conclude that entanglement between the atom and the pseudomodes is manifested only through two-way entanglement channels. A three-way entanglement is completely absent.

In Figs. 5(a) and 5(b), we plot the concurrences as functions of time for the weak and strong coupling regimes, respectively. In the weak coupling regime, where a trapping state is formed, entanglement at a very early stage builds up only between the atom and pseudomode two, which is responsible for the short-term storage of information. After reaching a peak, it starts decaying where at the same time entanglement between the atom and pseudomode one, which is responsible for the

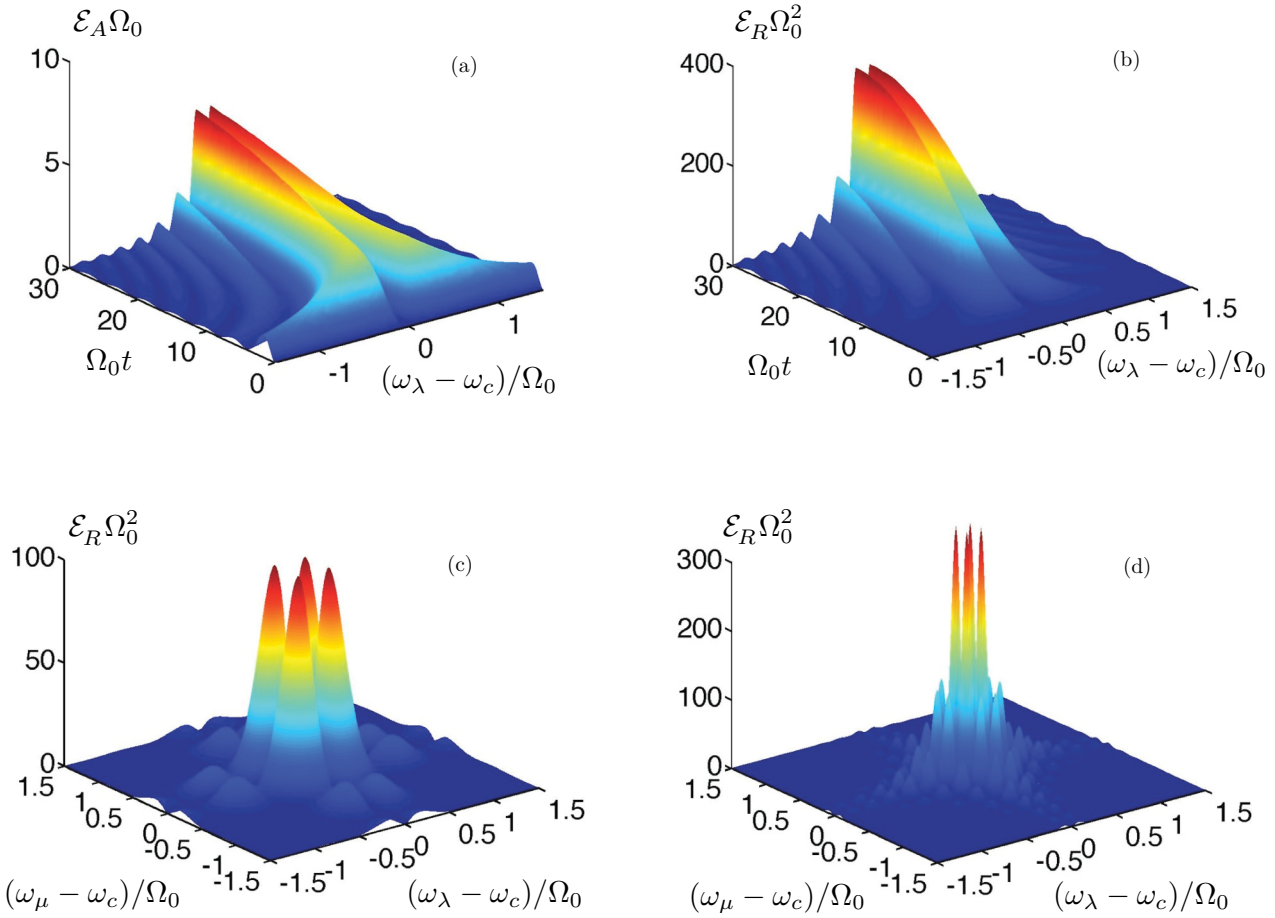

FIG. 6. (Color online) (a) The atom-modes density of entanglement $\mathcal{E}_A(\omega_\lambda,t)$ as a function of time and the mode frequency ω_λ, and (b) the density of entanglement $\mathcal{E}_R(\omega_\lambda,\omega_\mu,t)$ between a mode $\omega_\mu = \omega_c + 0.1\Omega_0$ and the rest of the reservoir modes as a function of time. Panels (c) and (d) are snapshots for the mode-mode density of entanglement $\mathcal{E}_R(\omega_\lambda,\omega_\mu,t)$ for $\Omega_0 t = 10$ and $\Omega_0 t = 30$, respectively. For all panels $\Gamma_1 = 10\Omega_0$, $\Gamma_2 = 0.2\Omega_0$, and $W_1 = 50W_2$.

long-term storage of information, slowly builds up and reaches a steady state. Thus, the trapping state is also an entangled state between the atom and the reservoir.

For the strong coupling regime, pseudomode one makes a negligible contribution in the entanglement dynamics. Pseudomode two has a strong contribution for short times, where the concurrence $C_{a,2}(t)$ quickly increases, and then follows a slowly decaying oscillation pattern. These oscillations are the signature of a Rabi splitting observed in the strong coupling regime [15]; see also the reservoir spectrum in Fig. 3(b).

B. Density of entanglement

In order to gain further insight into entanglement dynamics, we need to consider entanglement between the atom and each of the reservoir modes. For quantifying the distribution of entanglement between the atom and the individual reservoir modes, and among the reservoir modes, we use the density of entanglement [15]. The density of entanglement between the atom and modes with frequencies in an interval ω_λ to $\omega_\lambda + \mathrm{d}\omega_\lambda$ is

$$\mathcal{E}_A(\omega_\lambda,t) = 4|c_a(t)|^2 S(\omega_\lambda,t), \tag{26}$$

and the density of entanglement among the reservoir modes reads

$$\mathcal{E}_R(\omega_\lambda,\omega_\mu,t) = 2S(\omega_\lambda,t)S(\omega_\mu,t), \tag{27}$$

where $S(\omega_\lambda,t)$ is the reservoir spectrum.

In terms of these two distributions, the total entanglement or concurrence $C^2(t)$ for the atom and the reservoir modes is defined as the sum of an atom-modes contribution

$$C_A^2(t) = \int_{-\infty}^{\infty} d\omega_\lambda \mathcal{E}_A(\omega_\lambda,t), \tag{28}$$

and a reservoir contribution

$$C_R^2(t) = \int_{-\infty}^{\infty} d\omega_\lambda \int_{-\infty}^{\infty} d\omega_\mu \mathcal{E}_R(\omega_\lambda,\omega_\mu,t). \tag{29}$$

The total entanglement reads

$$C^2(t) = C_A^2(t) + C_R^2(t). \tag{30}$$

For the strong coupling regime, as shown earlier, the dynamics are similar to those for an atom coupled to a reservoir with a Lorentzian structure function. Thus, entanglement dynamics will be similar for the atom-reservoir system under consideration in Ref. [15]. The main feature for the reservoir density of entanglement is a pronounced Rabi splitting.

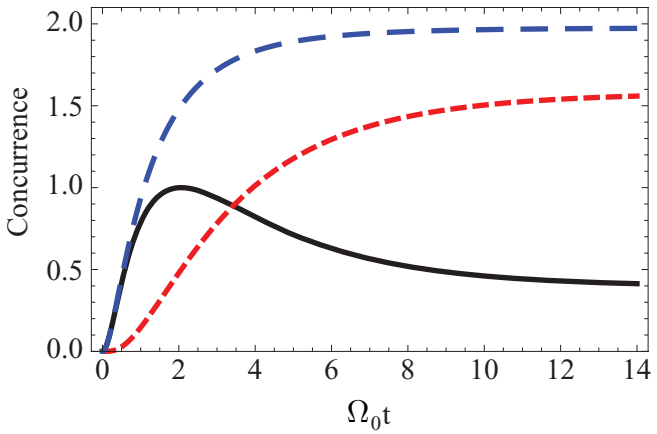

FIG. 7. (Color online) The concurrence $C_A^2(t)$ (black solid), $C_R^2(t)$ (red short-dashed) and the total concurrence $C^2(t)$ (blue dashed), for $\Gamma_1 = 10\Omega_0$, $\Gamma_2 = 0.2\Omega_0$, and $W_1 = 50W_2$.

Furthermore, this splitting results in decaying oscillations in the atom-modes density of entanglement.

On the other hand, for the weak coupling regime the dynamics are different. The formation of the trapping state is associated with a continuous population exchange between the atom and individual modes while the net flow of probability is equal to zero as discussed before. As a consequence, both entanglement distributions change in time, as can be seen in Fig. 6(a) for $\mathcal{E}_A(\omega_\lambda,t)$ and in Fig. 6(b) for $\mathcal{E}_R(\omega_\lambda,\omega_\mu,t)$. Both distributions do not reach a steady state in the long time limit. This feature for $\mathcal{E}_R(\omega_\lambda,\omega_\mu,t)$ is also evidenced in Figs. 6(c) and 6(d), where the density of entanglement for the reservoir modes is plotted for different times.

In contrast to this, due to population conservation and the fact that the net population exchange $Q(t)$ in the long time limit is zero, the total entanglement between the atom and the reservoir $C_A^2(t)$ is constant for $t \to \infty$. The same is true for the total entanglement for the reservoir modes $C_R^2(t)$ and the total entanglement $C^2(t)$. In Fig. 7, we plot $C_A^2(t)$, $C_R^2(t)$, and the total concurrence $C^2(t)$ for the weak coupling regime.

From this we see that at very early times, a rapid build up of entanglement takes place between the atom and the reservoir. Entanglement between the reservoir modes evolves at a much slower rate. Upon reaching a maximum, atom-reservoir entanglement follows a decay reaching a steady state at about the same time as the entanglement between the reservoir modes does. This point in time corresponds to the formation of the final trapping state between the atom and the reservoir.

V. CONCLUSIONS

In this work we have studied correlations and entanglement for an atom-photon bound state. Such states can be formed when an atom couples to a reservoir with a gap in its density of modes. Their main feature is that, in the long time limit, the system reaches a steady state where the initial atomic excitation energy is shared between the atom and the reservoir.

Despite the fact that for such a state no change is expected in the long time limit, a careful study of intrareservoir dynamics has revealed that this is not the case. For a reservoir with a single frequency gap in its structure function, we have shown that in the long time limit, the atom exchanges energy with individual modes, and though the net energy flow is zero, a permanent effective coupling between the modes is induced. As a result, the reservoir spectrum changes with time and a steady energy distribution is never reached.

The existence of the atom-photon bound state is explained, in terms of the pseudomode description, with the formation of a dark state by the atom and one of the pseudomodes, which are both coherently coupled to that pseudomode which connects to the rest of the environment. In general, the population trapping occurs in the weak coupling regime, whereas with strong coupling and no trapping, the dynamics within the environment begins to resemble the one obtained by single Lorentzian distribution. Furthermore, we have studied in the detail the entanglement dynamics between the atom and the pseudomodes, and within the environmental modes, highlighting several qualitative and quantitative differences between the weak and strong coupling regimes.

The results and methods used in this work can be extended and applied to systems where the reservoir density of modes has a broader gap or a more complicated structure. Such evolved reservoir structures can be encountered in photonic crystals or when considering the problem of atom-laser outcoupling from Bose-Einstein condensates.

ACKNOWLEDGMENTS

This work was supported by the Jenny and Antti Wihuri Foundation, Magnus Ehrnrooth Foundation, Vilho, Yrjö and Kalle Väisälä Foundation, the Academy of Finland (Project No. 259827), and the COST Action MP1006.

APPENDIX: SOLUTION OF THE SCHRÖDINGER EQUATION AND THE PSEUDOMODES METHOD

Starting with an atom initially excited and the reservoir in a vacuum state, the system's wave function for $t > 0$ will be

$$|\psi(t)\rangle = c_a(t)|1_a\rangle|\mathbf{0}\rangle + \sum_\lambda c_\lambda(t)|0_a\rangle|\psi_\lambda\rangle. \tag{A1}$$

The collective vacuum state for all reservoir modes ω_λ is

$$|\mathbf{0}\rangle = \prod_\lambda |0_\lambda\rangle, \tag{A2}$$

and the state with a single excitation in one of the reservoir modes is

$$|\psi_\lambda\rangle = |1_\lambda\rangle \prod_{k\neq\lambda} |0_k\rangle. \tag{A3}$$

At $t = 0$, we have that $c_a(0) = 1$ and $c_\lambda(0) = 0$.

The coefficients $c_a(t)$ and $c_\lambda(t)$ can be obtained by solving the Schrödinger equations

$$i\dot{\tilde{c}}_a(t) = \sum_\lambda g_\lambda e^{-i\delta_\lambda t}\tilde{c}_\lambda(t), \tag{A4a}$$

$$i\dot{\tilde{c}}_\lambda(t) = g_\lambda e^{i\delta_\lambda t}\tilde{c}_a(t), \tag{A4b}$$

where the detuning between the atomic transition and the mode λ is $\delta_\lambda = \omega_\lambda - \omega_0$. The amplitudes in the interaction picture are $\tilde{c}_a(t) = e^{i\omega_0 t}c_a(t)$ and $\tilde{c}_\lambda(t) = e^{i\omega_\lambda t}c_\lambda(t)$.

To derive $c_a(t)$ and $c_\lambda(t)$, one can numerically integrate Eqs. (A4a) and (A4b) using a discretization technique [9,16, 17] or by using the Laplace transform [20,22]. A different approach is that offered by the pseudomodes method [23,24]. The main feature of this technique is that the infinitely many equations for the reservoir modes can be replaced by a finite number of equations. Thus, the computational effort is substantially reduced. In addition to this, the pseudomodes method has provided an intuitive insight into non-Markovian dynamics, which are observed when an atom strongly couples to its environment [28].

When the reservoir structure function is analytic with a finite number of poles in the lower complex plane, Eqs. (A4a) and (A4b) can be replaced by a set of equivalent equations [23,24]. In this new set of equations, the atom couples to a finite set of fictitious modes, the pseudomodes, where each of these modes has a one-to-one correspondence to the poles of $D(\omega)$.

For the structure function $D(\omega)$ in Eq. (5), the analysis for arbitrary widths (Γ_1,Γ_2) and weights (W_1, W_2) was previously carried out; see Ref. [24]. Here we focus only on the perfect gap case, i.e., $D(\omega_c) = 0$, where the equations for the atomic excitation $c_a(t)$ and the two pseudomodes $a_1(t)$ and $a_2(t)$ are [24]

$$i\dot{c}_a(t) = \omega_0 c_a(t) + \Omega_0 a_2(t), \tag{A5a}$$

$$i\dot{a}_1(t) = \omega_c a_1(t) + \frac{\sqrt{\Gamma_1\Gamma_2}}{2} a_2(t), \tag{A5b}$$

$$i\dot{a}_2(t) = \left(\omega_c - i\frac{\Gamma_1+\Gamma_2}{2}\right) a_2(t) + \Omega_0 c_a(t) + \frac{\sqrt{\Gamma_1\Gamma_2}}{2} a_1(t). \tag{A5c}$$

These equations can be associated to the following master equation

$$\dot{\rho}(t) = -i\,[H_0, \rho(t)] - \frac{\Gamma_1+\Gamma_2}{2} \times [\hat{a}_2^\dagger \hat{a}_2 \rho(t) - 2\hat{a}_2 \rho(t) \hat{a}_2^\dagger + \rho(t)\hat{a}_2^\dagger \hat{a}_2], \tag{A6}$$

with the Hamiltonian

$$H_0 = \omega_0 |1_a\rangle\langle 1_a| + \omega_c(\hat{a}_1^\dagger \hat{a}_1 + \hat{a}_2^\dagger \hat{a}_2) + \Omega_0(\hat{a}_2^\dagger |0_a\rangle\langle 1_a| + \hat{a}_2 |1_a\rangle\langle 0_1|) + \frac{\sqrt{\Gamma_1\Gamma_2}}{2}(\hat{a}_1^\dagger \hat{a}_2 + \hat{a}_1 \hat{a}_2^\dagger), \tag{A7}$$

where $\hat{a}_1$ ($\hat{a}_1^\dagger$) and $\hat{a}_2$ ($\hat{a}_2^\dagger$) are the annihilation (creation) operators for the two pseudomodes, respectively.

The solution for the master equation (A6) reads

$$\rho(t) = \Pi_j(t) |0_a 0_1 0_2\rangle\langle 0_a 0_1 0_2| + |\tilde{\psi}(t)\rangle\langle\tilde{\psi}(t)|, \tag{A8}$$

where

$$|\tilde{\psi}(t)\rangle = c_a(t)|1_a 0_1 0_2\rangle + a_1(t)|0_a 1_1 0_2\rangle + a_2(t)|0_a 0_1 1_2\rangle. \tag{A9}$$

The vacuum state population $\Pi_j(t)$ is given by

$$\Pi_j(t) = \frac{\Gamma_1+\Gamma_2}{2}\int_0^t d\tau |a_2(\tau)|^2. \tag{A10}$$

The Fock states with zero or one excitation for the two pseudomodes are $|0_1\rangle$ ($|0_2\rangle$) and $|1_1\rangle$ ($|1_2\rangle$), respectively. From Eq. (A8) we see that the atom and the pseudomodes are in a mixed state.

Equations (A5a)–(A5c) are linear with time-independent coefficients and solutions can be easily obtained with the Laplace transform method. With the initial population for the atom being $c_a(0) = 1$, and both pseudomodes in a vacuum state, $a_1(0) = a_2(0) = 0$, we get for $c_a(t)$

$$c_a(t) = \frac{4e^{i\omega_0 t}}{4\Gamma^2+\Omega^2}\left\{\frac{\Gamma_1\Gamma_2}{4} + \frac{2\Omega_0^2}{\Omega} e^{-\Gamma t}\left[\Gamma \sin\left(\frac{\Omega t}{2}\right) + \frac{\Omega}{2}\cos\left(\frac{\Omega t}{2}\right)\right]\right\}, \tag{A11}$$

and for the pseudomodes

$$a_1(t) = -\frac{2\sqrt{\Gamma_1\Gamma_2}\Omega_0 e^{i\omega_0 t}}{(4\Gamma^2+\Omega^2)}\left\{1 - e^{-\Gamma t}\left[\cos\left(\frac{\Omega t}{2}\right) + \frac{2\Gamma}{\Omega}\sin\left(\frac{\Omega t}{2}\right)\right]\right\}, \tag{A12}$$

and

$$a_2(t) = -\frac{2i\Omega_0 e^{i\omega_0 t}}{\Omega}\sin\left(\frac{\Omega t}{2}\right) e^{-\Gamma t}. \tag{A13}$$

Here we consider only the resonant case $\omega_0 = \omega_c$. The decay rate Γ and the Rabi frequency Ω are

$$\Gamma = \frac{\Gamma_1+\Gamma_2}{4}, \tag{A14}$$

and

$$\Omega = \frac{1}{2}\sqrt{16\Omega_0^2 - (\Gamma_1-\Gamma_2)^2}. \tag{A15}$$

Substituting Eq. (A12) into (A10), we get for the vacuum state population

$$\Pi_j(t) = \frac{16\Gamma\Omega_0^2}{\Omega^2}\left[\frac{\Omega^2}{4\Gamma(4\Gamma^2+\Omega^2)} - \frac{e^{-2\Gamma t}}{4\Gamma} + \frac{\Gamma\cos(\Omega t) - \frac{\Omega}{2}\sin(\Omega t)}{(4\Gamma^2+\Omega^2)} e^{-2\Gamma t}\right]. \tag{A16}$$

Finally, using Eqs. (A1) and (A4b), we get the amplitudes $c_\lambda(t)$ for the reservoir modes

$$c_\lambda(t) = -\frac{4ie^{i\omega_\lambda t} g_\lambda}{4\Gamma^2+\Omega^2}\left\{\frac{\Gamma_1\Gamma_2}{2\delta_\lambda} e^{i\delta_\lambda t/2}\sin\left(\frac{\delta_\lambda t}{2}\right) + \frac{4\Omega_0^2(2\Gamma - i\delta_\lambda)}{4(\Gamma - i\delta_\lambda)^2+\Omega^2}\left[1 - e^{i\delta_\lambda t - \Gamma t}\cos\left(\frac{\Omega t}{2}\right)\right] + \frac{2\Omega_0^2(4(i\delta_\lambda\Gamma - \Gamma^2) + \Omega^2)}{\Omega(4(\Gamma - i\delta_\lambda)^2+\Omega^2)} e^{i\delta_\lambda t - \Gamma t}\sin\left(\frac{\Omega t}{2}\right)\right\}, \tag{A17}$$

where $\delta_\lambda = \omega_\lambda - \omega_c$ is the detuning between the λ mode and the gap frequency ω_c.

[1] L. Amico, R. Fazio, A. Osterloh, and V. Vedral, Rev. Mod. Phys. **80**, 517 (2008).
[2] R. Horodecki, P. Horodecki, M. Horodecki, and K. Horodecki, Rev. Mod. Phys. **81**, 865 (2009).
[3] M. A. Nielsen and I. L. Chuang, *Quantum Computation and Quantum Information* (Cambridge University Press, Cambridge, 2000).
[4] D. Leibfried, R. Blatt, C. Monroe, and D. Wineland, Rev. Mod. Phys. **75**, 281 (2003).
[5] F. Dalfovo, S. Giorgini, L. P. Pitaevskii, and S. Stringari, Rev. Mod. Phys. **71**, 463 (1999).
[6] A. J. Leggett, Rev. Mod. Phys. **73**, 307 (2001).
[7] J. M. Raimond, M. Brune, and S. Haroche, Rev. Mod. Phys. **73**, 565 (2001).
[8] B. T. H. Varcoe, S. Brattke, and H. Walther, New J. Phys. **6**, 97 (2004).
[9] P. Lambropoulos, G. M. Nikolopoulos, T. R. Nielsen, and S. Bay, Rep. Prog. Phys. **63**, 455 (2000).
[10] G. M. Nikolopoulos, P. Lambropoulos, and N. P. Proukakis, J. Phys. B **36**, 2797 (2003).
[11] C. Lazarou, G. M. Nikolopoulos, and P. Lambropoulos, J. Phys. B **40**, 2511 (2007).
[12] G. M. Nikolopoulos, C. Lazarou, and P. Lambropoulos, J. Phys. B **41**, 025301 (2008).
[13] N. I. Cummings and B. L. Hu, Phys. Rev. A **77**, 053823 (2008).
[14] J. Leandro and F. Semio, Opt. Comm. **282**, 4736 (2009).
[15] C. Lazarou, B. M. Garraway, J. Piilo, and S. Maniscalco, J. Phys. B **44**, 065505 (2011).
[16] G. M. Nikolopoulos, S. Bay, and P. Lambropoulos, Phys. Rev. A **60**, 5079 (1999).
[17] G. M. Nikolopoulos and P. Lambropoulos, Phys. Rev. A **61**, 053812 (2000).
[18] S. Bay, P. Lambropoulos, and K. Mølmer, Phys. Rev. A **55**, 1485 (1997).
[19] S. Bay and P. Lambropoulos, Opt. Commun. **146**, 130 (1998).
[20] S. John and T. Quang, Phys. Rev. A **50**, 1764 (1994).
[21] N. Vats and S. John, Phys. Rev. A **58**, 4168 (1998).
[22] A. G. Kofman, G. Kurizki, and B. Sherman, J. Mod. Opt. **41**, 353 (1994).
[23] B. M. Garraway, Phys. Rev. A **55**, 2290 (1997).
[24] B. M. Garraway, Phys. Rev. A **55**, 4636 (1997).
[25] V. Coffman, J. Kundu, and W. K. Wootters, Phys. Rev. A **61**, 052306 (2000).
[26] S. R. Entezar, Phys. Lett. A **373**, 3413 (2009).
[27] L. Jiang, S. Du, R.-G. Wan, J. Kou, H. Zhang, and H.-Z. Zhang, Opt. Comm. **284**, 2509 (2011).
[28] L. Mazzola, S. Maniscalco, J. Piilo, K.-A. Suominen, and B. M. Garraway, Phys. Rev. A **80**, 012104 (2009).
[29] I. E. Linington and B. M. Garraway, J. Phys. B **39**, 3383 (2006).
[30] J. Gambetta, T. Askerud, and H. M. Wiseman, Phys. Rev. A **69**, 052104 (2004).
[31] K. Luoma, K.-A. Suominen, and J. Piilo, Phys. Rev. A **84**, 032113 (2011).
[32] S. Hill and W. K. Wootters, Phys. Rev. Lett. **78**, 5022 (1997).
[33] W. K. Wootters, Phys. Rev. Lett. **80**, 2245 (1998).
[34] F. Mintert, A. R. Carvalho, M. Kus, and A. Buchleitner, Phys. Rep. **415**, 207 (2005).
[35] H. Barnum, E. Knill, G. Ortiz, R. Somma, and L. Viola, Phys. Rev. Lett. **92**, 107902 (2004).
[36] D. A. Meyer and N. R. Wallach, J. Math. Phys. **43**, 4273 (2002).
[37] S. J. Akhtarshenas, J. Phys. A: Math. Gen. **38**, 6777 (2005).